Supplementary materials

Hydrological connectivity can improve water quality and drive high variability of hydrochemistry: A study on a typical inland river in Xinjiang, China

Chuanxiu Liu [1,2], Yaning Chen[1, *], Zhi Li [1], Gonghuan Fang[1], Honghua Zhou[1], Wenjing Huang[1,2], Yongchang Liu[1 ,2], Xuanxuan Wang[1 ,2]

[1] State Key Laboratory of Desert and Oasis Ecology, Xinjiang Institute of Ecology and Geography, Chinese Academy of Sciences, Urumqi 830011, China

[2] College of Resources and Environment, University of China Academy of Sciences, Beijing 100049, China

[*] Corresponding author： Yaning Chen (chenyn@ms.xjb.ac.cn)

Text S1. Selection of hydrological connectivity thresholds

Using the Conefor plug-in (Conefor input) generated by Conefor Sensinode 2.6 in ArcGIS 10.2 software, to calculate the input files required for the hydrological connectivity index, including node files (water patches), connection files (connections between pairs of nodes described by Euclidean distances), and output the files in the form of tables. The integral index of connectivity (IIC) is calculated by Conefor Sensinode 2.6 software. The threshold distance of patch connectivity is required for the calculation. We have demonstrated that when the threshold reaches 20,000 m, most of the IIC index reach 1 and no longer change. The following distances have been tested for calculating the IIC in 1998 (dry year), 2003 (normal period), and 2010 (wet period) (Table.A2): 30m, 50m, 100m, 250m, 500m, 750m, 1000m, 1500m, 2000m, 2500m, 3000m, 4000m, 4500m, 5000m, 6000m, 7000m, and 8000m. The results showed that the IIC in BLB showed a consistent trend in different periods, which all increased with the increase of distance threshold (Figure.A5); when the distance threshold is between 30m and 2000 m, the IIC grows rapidly, and the connectivity of the patches in this interval is unstable and easily affected by the threshold; when the distance threshold is between2000 m and 8000 m, the IIC grows but tends to be stable, and the connectivity of the patches is more stable and less affected by the change of threshold. At a distance threshold above 20000 m, the IIC remains stable and the patches within the whole habitat are connected. In summary, the distance threshold for calculating hydrological connectivity has been set at 2000 m.

Text S2. Characteristics of water body changes in the BLB

The average annual total water body area (TWA) in the BLB from 1990 to 2019 was 1415.34 km^2 (Fig.A6a), accounting for 1.56% of the total basin area. The permanent water area (PWA) and seasonal water area (SWA) were 1100.39 km^2 and 314.95 km^2, respectively, accounting for 77.75% and 22.25% of the TWA, respectively (Fig. A6b). In 2019, there was a 509.94 km^2 fluctuating increasing trend in TWA compared to 1990 (Fig. A6a). The increase (about 610.67 km^2) was mainly concentrated in 1990-2000, and the decreasing occurring in 2000-2007. Noteworthy is that SWA increased at an average rate of 9.41 km^2 per year, with a total increase of 275.39 km^2 during the study period, whereas PWA increased only one-third the rate of SWA, with an average increase of 3.36 km^2 per year. By 2019, PWA had increased only 24.44% compared to 1990.

In general, PWA and SWA showed increases like TWA. These were mainly concentrated in 1990-2000 and rose 252.881 km^2 and 357.78 km^2, respectively. PWA continued to increase at a rate of 2.89 km^2/yr in 2000-2019, while SWA decreased at a rate of 1.70 km^2/yr. Figure 3c shows that the area of land-to-water conversion over the past 30 years was 1599.7 km^2. The largest conversion was to SWA (around 1199.47 km^2), while the area converted from SWA to land was also relatively large (about 871.80 km^2). The conversion of PWA to land was mainly concentrated in 2000-2005, with the conversion amount topping 124.47 km^2. The rest of the time period saw land converted to PWA.

Spatially, the distribution of water bodies in the BLB is diverse. The water bodies

were mainly spread across higher altitudes in the KDH and the oasis area in the KKH, while there were very few water bodies distributed in KQH, especially in the lower reaches of the Konqi River. As shown in Figs. A7a and b, the increase in water body area mainly occurred around Bosten Lake and in the main stream of the Kaidu River (Figs. A7c-h). The water body area around Bosten Lake showed varying degrees of increasing changes during most of the study period, except for 2000-2005. Specifically, the water body area around Bosten Lake increased around 455.30 km^2 from 1990 to 2000, which represents 74.56% of the change in this period and 89.29% of the total change in TWA, respectively. The reason for this phenomenon is that as the climate warms, there is an increase in ice and snow meltwater along with enhanced river runoff recharge in the KDH, which belongs to the high-altitude mountainous region. This leads to an increase in the upstream watershed area (Fan et al., 2021; Deng et al., 2015). Meanwhile, the river's middle reaches, which belong to the oasis ecosystem, are a water-consuming area with a complex river-lake-reservoir network system (Ariken et al., 2020; Li et al., 2015). Water consumption from human activities and ecological water demand dissipation decreases water resources and results in low runoff and serious desertification in the lower reaches of the Konqi River.

The largest permanent water patch in the BLB is the Bosten Lake, with an annual average area of 968.98 km^2, which accounts for 87.87% of the PWA. BLA had a significant temporal variation characteristic (Fig.A1). Bosten Lake area (BLA) increased rapidly at a rate of 9.6 km^2/yr from 1990 to 2000, approximately 108.64 km^2. while from 2000 to 2007, BLA decreased rapidly, averaging 20 km^2 per year, and BLA

reached its lowest value of 899.31 km^2 in 2007 and then increased rapidly at a rate of 11.22 km^2/yr to a maximum value of 1041.08km^2 (2018). The fluctuation trend of BLL was generally consistent with the BLA (Fig.A1). Specifically, Bosten Lake level (BLL) shows a characteristic of rising (1990-2002), then falling (2003-2013) and then rising (2013-2019), with a maximum value of 1048.65m in 2002 and a minimum value of 1045.12m in 2013.

The annual average concentration of TDS reached 1308.67 mg/L, which was brackish. The attainment rate of the freshwater standard was 10.52%, with its highest concentration up to 1779.13 mg/L occurring in 2013. Only in 2016 and 2019 did it reach the freshwater standard (< 1000 mg/L) (Table.A4). At the same time, however, its concentration had the fastest interannual decline rate (4.82 mg/L/y) and a high degree of variability (SD = 224) (Table.A5). Therefore, the water environment management of Bosten Lake should focus on COD, TN, and TDS pollution. Additionally, the management of agricultural activities around the lake should be strengthened and the hydrological connectivity of the surrounding canals should be increased to increase the hydrodynamics of the lake and enhance its self-purification capacity.

Text.S3. Water quality change characteristics from 2001-2019

In general, DO facilitates the dissolution of various pollutants in a water body so that it can be purified more quickly (Baxa et al., 2021). The concentration of COD did not exceed the surface water category III standard from 2001 to 2019, as shown in Fig. 6a, but its concentration was in a decreasing trend. Moreover, the mean concentration of NH_3-N was 0.12 mg/L, which is compliant with the standard of surface water

category III (≤ 1 mg/L). The attainment rate is 100%, while its concentration shows an increasing trend with a large dispersion (CV = 0.56) (Fig. 5d and Table.A5). This further indicates that although there is no DO or NH_3-N pollution in Bosten Lake at present, the concentration of these two substances will increase with the impact of human activities. Moreover, because the result will likely cause water pollution, preventative measures should be taken in advance.

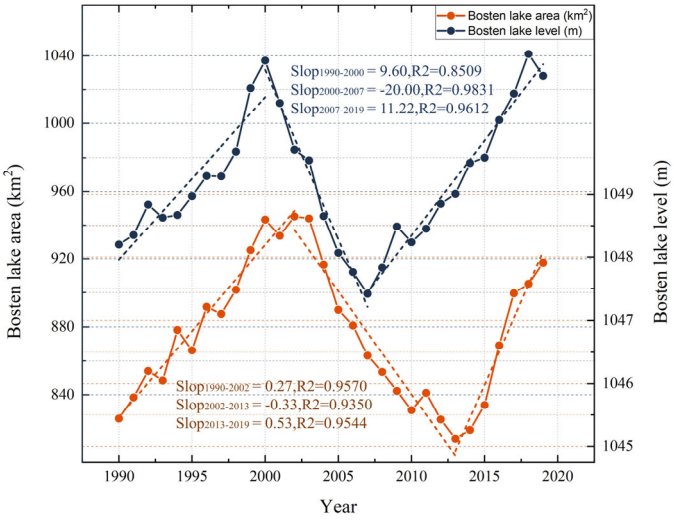

Figure S1. Change trend of Bosten lake water area and level change from 1990 to 2019.

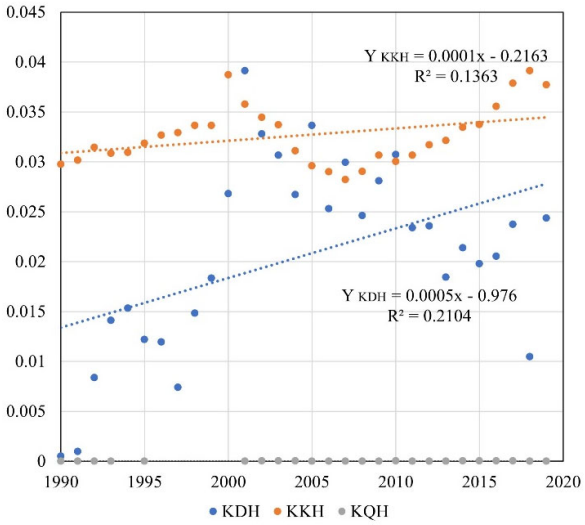

Figure S2. Time series and trends of yearly IIC from 1990-2019 of each sub-basin.

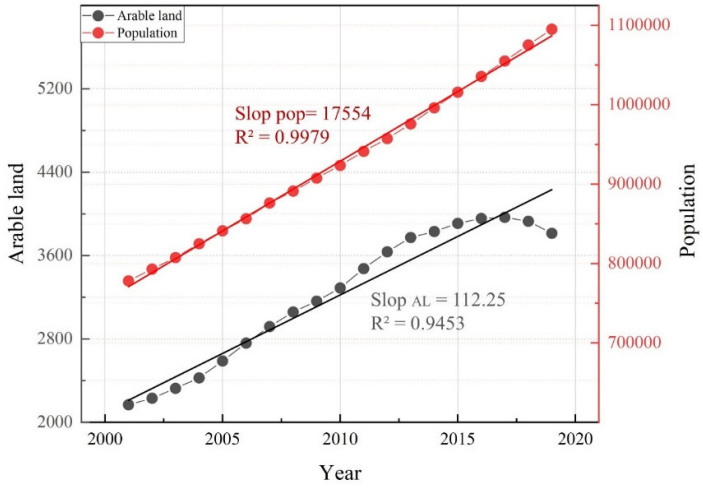

Figure S3. Arable land area and population change of BLB.

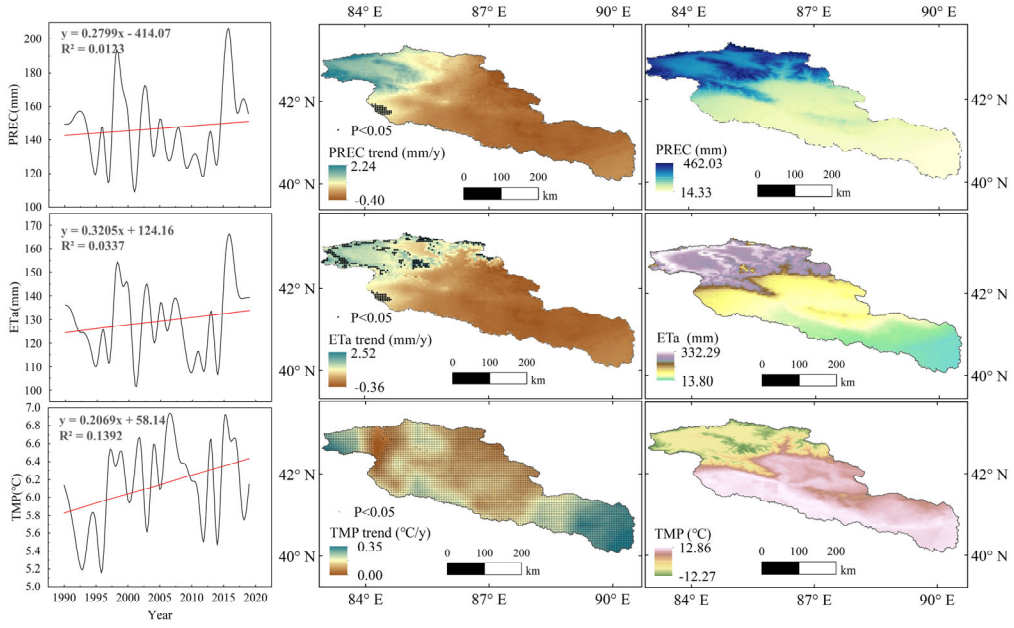

Figure S4. Temporal and spatial variations of PREC, ETa and TMP and their significance tests. Black dots represent passing the $P < 0.05$ test.

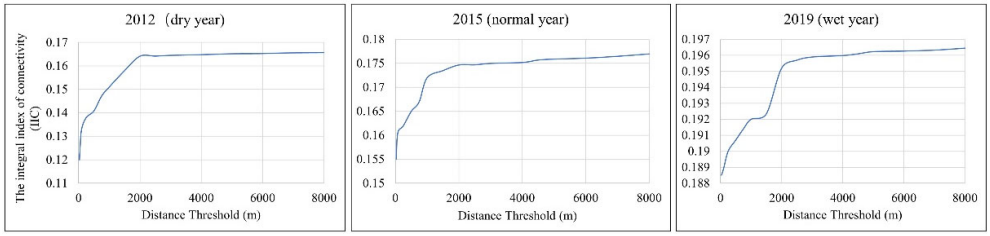

Figure S5. Variation of IIC at different distance thresholds

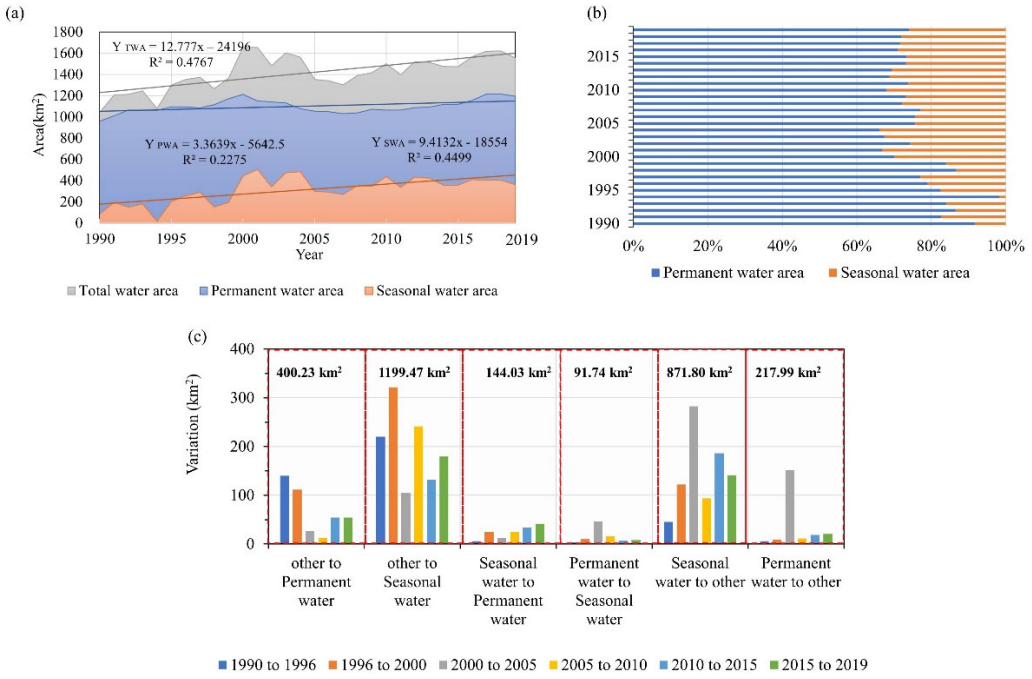

Figure S6. 1990-2019 BLB (a) variations of TWA, PWA, SWA, (b) percentage of PWA and SWA, and (c) conversion between different types of water bodies.

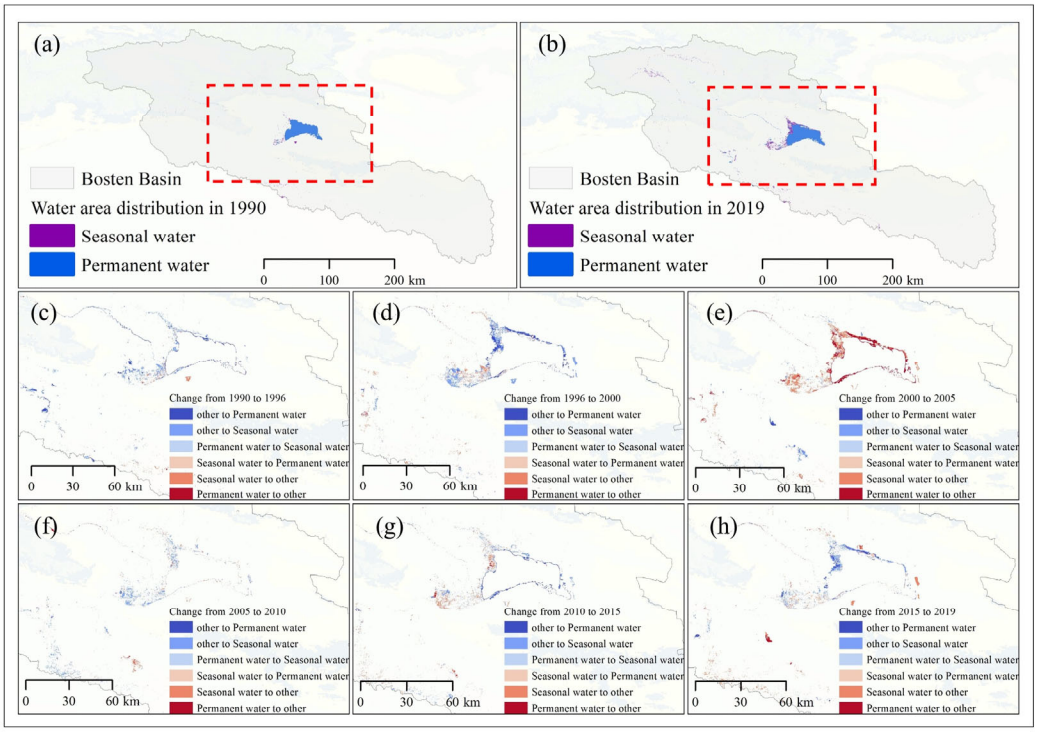

Figure S7. (a)Water area distribution in 1990, (b) water area distribution in 2019, (c)water area change from 1990 to 1996, (d) water area change from 1996 to 2000, (e) water area change from 2000 to 2005, (f) water area change from 2005 to 2010, (g) water area change from 2010 to 2015, (h) water area change from 2015 to 2019.

Table S1. Details of the data source for this article

Data	Source	Data length
Water area	JRC Yearly/Monthly Water Classification History, v1.3 (https://earthengine.google.com/)	1984 to 2019
Bosten Lake level	Xinjiang Tarim River Basin Authority (http://www.tahe.gov.cn/cs.htm)	1990-2019
Precipitation	TerraClimate（http://www.climatologylab.org/）	1958 to 2020
Actual Evapotranspiration	TerraClimate（http://www.climatologylab.org/）	1958 to 2020
Temperature	1-km monthly mean temperature dataset for china（https://data.tpdc.ac.cn/zh-hans/data/71ab4677-b66c-4fd1-a004-b2a541c4d5bf/?q=1km）	1901-2020

Soil Moisture	TerraClimate（http://www.climatologylab.org/）	1958 to 2020
NDVI	Google Earth Engine (https://developers.google.com/s/results/earth-engine/datasets?q=MOD13Q1.006%20Terra%20Vegetation%20Indices%2016-Day%20Global%20250m)	2000-2020
Population	WorldPop Global Project Population Data: Estimated Residential Population per 100x100m Grid Square (https://earthengine.google.com/)	2000 to 2020
Arable area	MCD12Q1.006 MODIS Land Cover Type Yearly Global 500m(https://earthengine.google.com/)	2001 to 2020

Table S2. Classification results of wet, dry and normal years from 1990 to 2019.

Year	Percentage of runoff anomaly	Type	Year	Percentage of runoff anomaly	Type
1990	-23	Dry Year	2005	-8	Normal Year
1991	-12	Dry Year	2006	4	Normal Year
1992	-12	Dry Year	2007	-2	Normal Year
1993	-18	Dry Year	2008	-3	Normal Year
1994	7	Normal Year	2009	-1	Normal Year
1995	-25	Dry Year	2010	14	Wet Year
1996	5	Normal Year	2011	4	Normal Year
1997	4	Normal Year	2012	-17	Dry Year
1998	6	Normal Year	2013	-21	Dry Year
1999	25	Wet Year	2014	-22	Dry Year
2000	30	Wet Year	2015	-3	Normal Year
2001	10	Wet Year	2016	1	Normal Year
2002	47	Wet Year	2017	9	Normal Year
2003	5	Normal	2018	-1	Normal

		Year			Year
2004	10	Dry Year	2019	26	Wet Year

Note: Classification standard：Annual runoff anomaly percentage ≥ 10 is a wet year, ≤ -10 is a dry year.

Table S3. Chinese Environmental Quality for Surface Water III Standard（GB3838-2002）

Index	Standard value of water quality classification (mg/L)				
	I	II	III	IV	V
DO	≥7.5	≥6	**≥5**	≥3	≥2
COD_{MN}	≤2	≤4	**≤6**	≤10	≤15
COD	≤15	≤15	**≤20**	≤30	≤40
BOD_5	≤3	≤3	**≤4**	≤6	≤10
TP (lake)	≤0.01	≤0.025	**≤0.05**	≤0.1	≤0.2
TN	≤0.2	≤0.5	**≤1.0**	≤1.5	≤2.0
NH_3-N	≤0.15	≤0.5	**≤1.0**	≤1.5	≤2

Note: Surface water quality standards of Bosten Lake Basin require a Class III standard.

Table S4. Standard for classification of fresh and salt water

Classification	Fresh water	Brackish water	Salt water	Brine
TDS (mg/L)	0-1000	1000-3000	3000-10000	＞10000

Table S5. Characteristic values of interannual variation of water quality indexes

Index	The proportion of III standards (%)	Slop （mg/L/y）	Max （mg/L）	Min （mg/L）	Mean （mg/L）	Standard Deviation (SD)	Coefficient of Variance (CV)
DO	100	-0.0096	9.1614	6.3832	7.5242	0.6917	0.0919
COD_{MN}	100	-0.04	5.7049	2.7975	4.8463	0.6623	0.1367
COD	36.84	-0.1078	28.6824	18.1261	23.4083	3.0854	0.1318
BOD_5	100	-0.0631	2.3104	0.7370	1.6535	0.5123	0.3098
TP	100	-0.0059	0.5081	0.0085	0.0168	0.0085	0.5082
TN	94.74	-0.0008	1.0020	0.6258	0.8301	0.0960	0.1157
NH_3-N	100	0.0081	0.5567	0.0207	0.1232	0.0686	0.5567
TDS	10.52	-4.8167	1799.1266	890	1308.6739	224.1184	0.1713

Table S6. Multiple stepwise regression results

Factor	Coefficient ($\times 10^{-3}$)	P
Precipitation	**6.74**	0.05

Temperature	-1.17	1
Actual evapotranspiration	**-8.79**	0.05
Arable land	**-5.07**	0
Population	**4.01**	0

Note: bolded indicates passing significance test.

Table S7. Water System connectivity Project of BLB

Year	Details	Water volume
1990	The third diversion hub of the Konqi River was completed.	/
1992	Integrated management of reservoirs - water towers - main canals.	/
1995-2005	River dredging, diversion hub and artificial canal system construction.	/
2014-2016	Huangshui River Diversion Project	/
2016-2020	In order to solve the problems such as the downstream disconnection of the Konqi River, there are four times ecological water deliveries to the Konqi River.	$4.89\times10^8m^3$
2018	Ecological water transfer from Huangshui River into Bosten Lake.	$1.14\times10^8m^3$
2019	Implementation of water transfer project from the Kaidu River to the Huangshui River, which linked the Kaidu River, the Huangshui River and Bosten Lake.	$2.0043\times10^8m^3$
2020	The project of transferring water from Kaidu River to Huangshui River was implemented to strengthen the water system connection between Kaidu River, Huangshui River and Bosten Lake.	$1.648\times10^8m^3$

References

Ariken, M., Zhang, F., Liu, K., Fang, C., Kung, H.-T., 2020. Coupling coordination analysis of urbanization and eco-environment in Yanqi Basin based on multi-source remote sensing data. Ecological Indicators 114, 106331. https://doi.org/10.1016/j.ecolind.2020.106331

Deng, H., Chen, Y., Wang, H., Zhang, S., 2015. Climate change with elevation and its potential impact on water resources in the Tianshan Mountains, Central Asia. Global and Planetary

Change 135, 28–37. https://doi.org/10.1016/j.gloplacha.2015.09.015

Fan, M., Xu, J., Chen, Y., Li, W., 2021. Modeling streamflow driven by climate change in data-scarce mountainous basins. Science of The Total Environment 790, 148256. https://doi.org/10.1016/j.scitotenv.2021.148256

Li, N., McLaughlin, D., Kinzelbach, W., Li, W., Dong, X., 2015. Using an ensemble smoother to evaluate parameter uncertainty of an integrated hydrological model of Yanqi basin. Journal of Hydrology 529, 146–158. https://doi.org/10.1016/j.jhydrol.2015.07.024